NEW GUIDELINES

Dear Author,

Please correct your galley proofs carefully and return them within 24–48 hours to aicheproof@wiley.com.

This will be your only chance to review these proofs. Please note that the volume and page numbers shown on the proofs are for position only.

The editors reserve the right to publish your article without your corrections if they are not received in time.

Please annotate all corrections on the supplied PDF.

To avoid commonly occurring errors, please ensure that the following important items are correct in your proofs (Please note that once your article has been published online, no further corrections can be made):

☐ Names of all authors present and spelled correctly (IMPORTANT: The addition or deletion of author names in proofs is strictly prohibited and may result in the suspension or termination of your article's production.)

☐ Addresses and postcodes correct

☐ E-mail address of corresponding author correct and current

☐ Title of article correct

☐ All figures included and in the correct order

☐ All tables and equations correct (symbols and superscripts)

☐ All queries (included on the last page) answered

Note: the resolution of the figures in the PDF proofs is intentionally of lower quality to facilitate internet delivery. These images will appear at higher resolution and sharpness in the printed article.

Reprint Purchases: Should you wish to purchase additional copies of your article, please click on the link and follow instructions provided:
https://caesar.sheridan.com/reprints/redir.php?pub=10089&acro=AIC

USING e-ANNOTATION TOOLS FOR ELECTRONIC PROOF CORRECTION

Required software to e-Annotate PDFs: Adobe Acrobat Professional or Adobe Reader (version 11 or above). (Note that this document uses screenshots from Adobe Reader DC.)
The latest version of Acrobat Reader can be downloaded for free at: http://get.adobe.com/reader/

Once you have Acrobat Reader open on your computer, click on the Comment tab (right-hand panel or under the Tools menu).

This will open up a ribbon panel at the top of the document. Using a tool will place a comment in the right-hand panel. The tools you will use for annotating your proof are shown below:
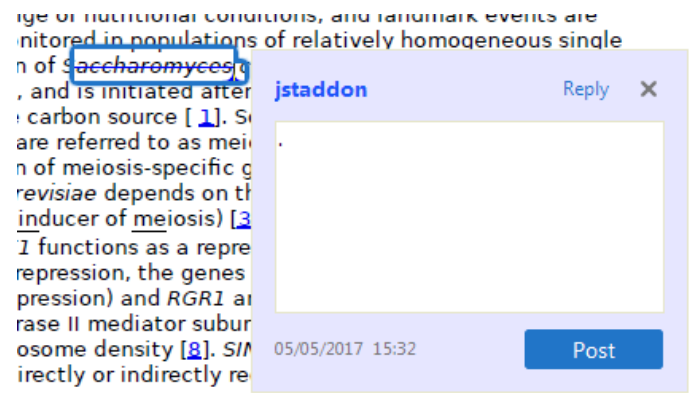
Export PDF	⌄
Create PDF	⌄
Edit PDF	⌄
Comment	

---
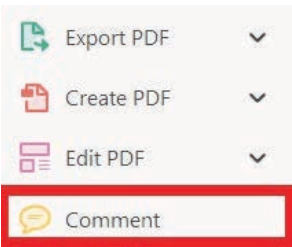
1. Replace (Ins) Tool – for replacing text.

Strikes a line through text and opens up a text box where replacement text can be entered.
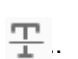
How to use it:

- Highlight a word or sentence.
- Click on ⊤̣ .
- Type the replacement text into the blue box that appears.

ige of nutritional conditions, and landmark events are
nitored in populations of relatively homogeneous single
n of *Saccharomyces* c
, and is initiated after
e carbon source [1]. S
are referred to as mei
n of meiosis-specific g
revisiae depends on th
inducer of meiosis) [3
1 functions as a repre
repression, the genes
pression) and *RGR1* a
rase II mediator subur
osome density [8]. *SIM*
irectly or indirectly re

jstaddon   Reply ✕
.

05/05/2017 15:32   Post

---

2. Strikethrough (Del) Tool – for deleting text.

Strikes a red line through text that is to be deleted.

How to use it:

- Highlight a word or sentence.
- Click on ⊤̅ .
- The text will be struck out in red.

experimental data if available. For ORFs to be
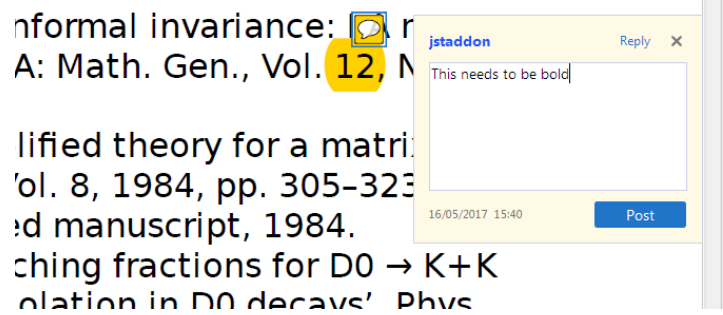had to meet all of the following criteria:

1. Small size (35–250 amino acids).
2. Absence of similarity to known proteins.
3. Absence of functional data which could n
   the real overlapping gene.
4. Greater than 25% overlap at the N-termin
   terminus with another coding feature; ove
   both ends; or ORF containing a tRNA.

---

3. Commenting Tool – for highlighting a section to be changed to bold or italic or for general comments.

Use these 2 tools to highlight the text where a comment is then made.

How to use it:

- Click on ✎ .
- Click and drag over the text you need to highlight for the comment you will add.
- Click on 💬 .
- Click close to the text you just highlighted.
- Type any instructions regarding the text to be altered into the box that appears.

nformal invariance: 💬 n
A: Math. Gen., Vol. 12, N

lified theory for a matri
ol. 8, 1984, pp. 305–323
ed manuscript, 1984.
ching fractions for D0 → K+K
olation in D0 decays', Phys

jstaddon   Reply ✕
This needs to be bold

16/05/2017 15:40   Post

---

4. Insert Tool – for inserting missing text at specific points in the text.

Marks an insertion point in the text and opens up a text box where comments can be entered.

How to use it:

- Click on ⊤̭ .
- Click at the point in the proof where the comment should be inserted.
- Type the comment into the box that appears.

Meiosis has a central role in the sexual reproduction of nearly all
eukaryotes *Saccharom*   or det
analysis of meiosis, esp   e trigg
by a simple change of n   ts are
conveniently monitored   Yeast,   us sin
cells. Sporulation of *Sac*   ne typ
cell, the a/α cell, and is   the a
of a fermentable carbor   only d
sporulation and are refe   c gen
2b]. Transcription of me   tion o
meiosis, in *S. cerevisiae*   ional
activator, *IME1* (inducer   e pro
of the gene *RME1* functi   DNA-k
Rme1p to exert repressi   ve re
of GAL1 gene expression) and *RGR1* are required [1, 2, 3, 2]. These ge

jstaddon   Reply ✕

05/05/2017 15:57   Post

5. Attach File Tool – for inserting large amounts of text or replacement figures.

Inserts an icon linking to the attached file in the appropriate place in the text.

How to use it:

- Click on .

- Click on the proof to where you'd like the attached file to be linked.
- Select the file to be attached from your computer or network.
- Select the colour and type of icon that will appear in the proof. Click OK.

The attachment appears in the right-hand panel.

:hondrial preparatior
ative damage injury
1e extent of membra
1, malondialdehyde (
(TBARS) formation.
urad by high parform

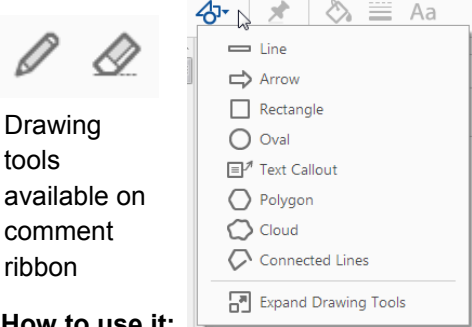**6. Add stamp Tool – for approving a proof if no corrections are required.**

Inserts a selected stamp onto an appropriate place in the proof.

How to use it:

- Click on .

- Select the stamp you want to use. (The Approved stamp is usually available directly in the menu that appears. Others are shown under *Dynamic*, *Sign Here*, *Standard Business*).

- Fill in any details and then click on the proof where you'd like the stamp to appear. (Where a proof is to be approved as it is, this would normally be on the first page).

)r the business cycle, starting with the
. on perfect competition, constant ret
production. In this environment goods
extra re fixed below the of market
he **APPROVED** total p
etermined by the model. The New-K¢yn
otaki (1987), has introduced produc
general equilibrium models with nomin
nd and supply shocks. Most of this literat

7. Drawing Markups Tools – for drawing shapes, lines, and freeform annotations on proofs and commenting on these marks.

Allows shapes, lines, and freeform annotations to be drawn on proofs and for comments to be made on these marks.

Drawing tools available on comment ribbon

- Line
- Arrow
- Rectangle
- Oval
- Text Callout
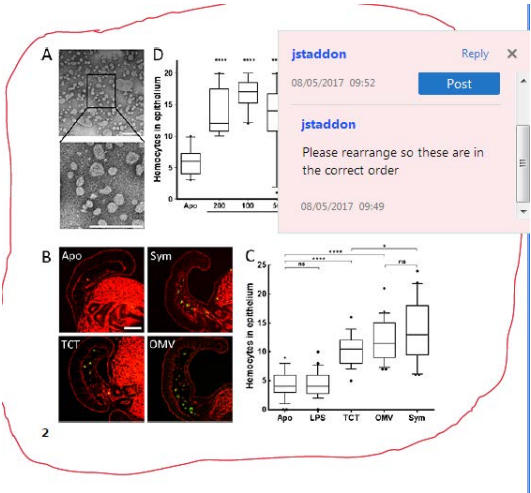- Polygon
- Cloud
- Connected Lines
- Expand Drawing Tools

How to use it:

- Click on one of the shapes in the Drawing Markups section.
- Click on the proof at the relevant point and draw the selected shape with the cursor.
- To add a comment to the drawn shape, right-click on shape and select *Open Pop-up Note.*
- Type any text in the red box that appears.

jstaddon   Reply X
08/05/2017 09:52   Post

jstaddon
Please rearrange so these are in the correct order
08/05/2017 09:49

For further information on how to annotate proofs, click on the Help menu to reveal a list of further options:

Help

Online Support   F1

Welcome...

(?) Learn Adobe Acrobat Reader DC...

About Adobe Acrobat Reader DC...

About Adobe Plug-Ins...

Generate System Report...

Repair Installation

Check for Updates...
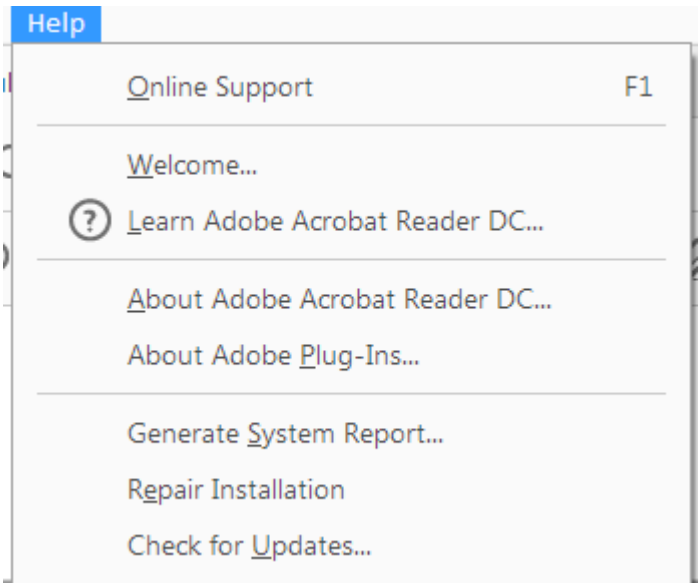
WILEY

COLOR REPRODUCTION IN YOUR ARTICLE

Color figures were included with the final manuscript files that we received for your article. Because of the high cost of color printing, we can only print figures in color if authors cover the expense. **The charge for printing figures in color is $700 per figure.**

Please indicate if you would like your figures to be printed in color or black and white. Color images will be reproduced online in *Wiley Online Library* at no charge, whether or not you opt for color printing.

Failure to return this form will result in the publication of your figures in black and white.

JOURNAL _____ VOLUME _____ ISSUE _____

TITLE OF MANUSCRIPT _____

MS. NO. _____   NO. OF COLOR PAGES _____   AUTHOR(S) _____

☐   Please print my figures in black and white

☐   Please print my figures in color $ _____

BILL TO:
Name _____

Institution _____

Address _____

_____

Purchase Order No. _____

Phone _____

_____

Fax _____

E-mail _____

WILEY

Author Query Form

Journal: AIC

Article: 16217

Dear Author,

During the copyediting of your manuscript the following queries arose.

Please refer to the query reference callout numbers in the page proofs and respond to each by marking the necessary comments using the PDF annotation tools.

Please remember illegible or unclear comments and corrections may delay publication.

Many thanks for your assistance.

Query References	Query	Remarks?
AQ1	AUTHOR: Please provide author affiliations and corresponding details are correct.	
AQ2	AUTHOR: Please confirm that given names (red) and surnames/family names (green) have been identified correctly.	

Funding Info Query Form

Please confirm that the funding sponsor list below was correctly extracted from your article: that it includes all funders and that the text has been matched to the correct FundRef Registry organization names. If a name was not found in the FundRef registry, it may be not the canonical name form or it may be a program name rather than an organization name, or it may be an organization not yet included in FundRef Registry. If you know of another name form or a parent organization name for a "not found" item on this list below, please share that information.

FundRef name	FundRef Organization Name
Shanghai Natural Science Foundation	Beijing Municipal Natural Science Foundation
	Guandong Natural Science Foundation
	National Natural Science Foundation of China
	Natural Science Foundation of Anhui Province
	Natural Science Foundation of Beijing Municipality
	Natural Science Foundation of Chongqing
	Natural Science Foundation of Fujian Province
	Natural Science Foundation of Gansu Province
	Natural Science Foundation of Guangxi Province
	Natural Science Foundation of Guizhou Province
	Natural Science Foundation of Hainan Province
	Natural Science Foundation of Hebei Province
	Natural Science Foundation of Heilongjiang Province
	Natural Science Foundation of Henan Province
	Natural Science Foundation of Hubei Province
	Natural Science Foundation of Huizhou University

Natural Science Foundation of Inner Mongolia	
Natural Science Foundation of Jiangsu Province	
Natural Science Foundation of Jiangxi Province	
Natural Science Foundation of Jilin Province	
Natural Science Foundation of Liaoning Province	
Natural Science Foundation of Ningbo	
Natural Science Foundation of Ningbo Municipality	
Natural Science Foundation of Ningxia Province	
Natural Science Foundation of Shaanxi Province	
Natural Science Foundation of Shandong Province	
Natural Science Foundation of Shanghai	
Natural Science Foundation of Shanxi Province	
Natural Science Foundation of Tianjin City	
Natural Science Foundation of Xinjiang Province	
Natural Science Foundation of Yunnan Province	
Natural Science Foundation of Zhejiang Province	
Natural Science Foundation ofÂ Hunan Province [NOT FOUND IN FUNDREF REGISTRY]	
Shanghai Rising-Star Program	Construct Program of the Key Discipline in Hunan Province Illinois Program for Research in the Humanities, University of Illinois at Urbana-Champaign Program for New Century Excellent Talents in University [NOT FOUND IN FUNDREF REGISTRY]
Open Project of State Key Laboratory of Chemical Engineering	[NOT FOUND IN FUNDREF REGISTRY]
111 Project of the Ministry of Education of China	[NOT FOUND IN FUNDREF REGISTRY]
Natural Science Foundation of Shanghai	Natural Science Foundation of Shanghai

REACTION ENGINEERING, KINETICS AND CATALYSIS

SbO$_x$-Promoted Pt Nanoparticles Supported on CNTs as Catalysts for Base-Free Oxidation of Glycerol to Dihydroxyacetone

Xuezhi Duan [ID], **Yanfang Zhang**, **Minjian Pan**, **Hua Dong**, **Bingxu Chen**, **Yuanyuan Ma**, **Gang Qian**, and **Xinggui Zhou** [ID]

State Key Laboratory of Chemical Engineering, East China University of Science and Technology, 130 Meilong Road, Shanghai 200237, China

Jia Yang and **De Chen** [ID]

Dept. of Chemical Engineering, Norwegian University of Science and Technology, Trondheim 7491, Norway

Understanding of selective base-free oxidation of glycerol to dihydroxyacetone (DHA) over Pt-based catalysts is of paramount scientific and industrial importance. In this work, a comparative study between differently sized SbO$_x$-promoted and unpromoted Pt/CNTs catalysts is carried out to decouple the promoter effects from the metal size effects. The introduction of SbO$_x$ appears to enhance both the glycerol oxidation activity and the DHA selectivity, and the largely sized promoted Pt/CNTs catalysts afford a relatively high DHA yield and less C–C bond cleavage. X-ray photoelectron spectroscopy measurements reveal that the Sb species are mainly in the form of SbO$_x$, and the differently sized promoted catalysts show similar metal binding energies. Furthermore, theoretical studies on the promotional effects of SbO$_x$ are carried out by DFT calculations. It is found that the presence of the promoter on the catalyst surface favors the preferential activation of the secondary hydroxyl group. © 2018 American Institute of Chemical Engineers *AIChE J*, 00: 000–000, 2018

Keywords: base-free oxidation of glycerol, dihydroxyacetone, SbO$_x$ promoted Pt/CNTs catalyst, size effects, promoter effects

Introduction

Selective catalytic oxidation of glycerol, using air or oxygen instead of costly and polluting stoichiometric oxidants, has attracted tremendous attention from both economic and environmental perspectives.[1–3] This process initially proceeds by means of not only the oxidation of the primary hydroxyl group to form glyceraldehyde (GLYD), but also that of the secondary hydroxyl group to form dihydroxyacetone (DHA) used as a tanning agent in the cosmetics industry and building blocks for degradable polymers.[4] Previous studies[5–8] demonstrated that the presence of base is beneficial for the glycerol oxidation because of its promotional effect on the H-abstraction of the hydroxyl groups being the rate limiting step, but detrimental to produce the targeted DHA product, e.g., the selectivity to DHA even being zero, because of that on the interconversion between the DHA and the GLYD. Interestingly, the use of base-free conditions has been found to enhance the

selectivity to DHA.[9–12] Therefore, we focus our attention on base-free oxidation of glycerol with the aim to maximize the DHA production.

For the base-free oxidation of glycerol, various carbon supported catalysts[11–16] have been widely studied, because the carbon supports not only endow the catalyst with an effective electron transfer system, but also exhibit high resistance to acidic/basic environments as well as unique and tunable surface chemistry and textural properties.[17–19] For example, Hutchings and co-workers reported that activated carbon supported Au catalysts are totally inactive.[14] Kimura et al. found that compared to charcoal supported Pd, Ru, and Re catalysts, Pt/charcoal catalysts show higher DHA yield, e.g., 4% at glycerol conversion of 37%.[12] Similarly, Garcia et al. revealed that the Pt/C catalyst exhibits six times higher reaction rate and 1.5 times higher DHA yield than the Pd/C catalyst, where the maximum DHA yield over the Pt/C catalyst by optimizing the reaction conditions is 12%.[13] Recently, the researchers further explored the effects of the Pt particle sizes and electronic properties on the DHA selectivity and yield.[11,20–22] However, in these studies, limited improvements in the DHA selectivity (<20%) and yield (<15%) were achieved. In other words, only optimizing the platinum particle size and electronic properties as well as the reaction conditions is not very effective to obtain desirable DHA selectivity and yield.

Interestingly, the introduction of appropriate promoters (e.g., Bi and Sb) into the Pt/C catalysts has been demonstrated to give rise to significantly improved reactivity to DHA.[12,13,23–25] However, the DHA selectivity over the Pt-Bi/C catalyst underwent dramatic decrease from 87 to 36% when the conversion increased from 10 to 90%.[24] In comparison with the Bi promoter, the introduction of Sb promoter gave rise to slow decrease in the DHA selectivity from 81 to 51% as the conversion increased from 10 to 90%,[25] suggesting that the Pt–Sb/C catalyst is a promising candidate for the selective base-free oxidation of glycerol to DHA. Therefore, an attempt is necessary to unravel the crucial role of the Sb promoter in the base-free oxidation of glycerol to DHA and then guide the rational design and optimization of Pt–Sb/C catalysts.

In this work, we focus on understanding of the promotional effects of antimony in Pt–Sb supported on carbon nanotubes (CNTs) catalyzed base-free oxidation of glycerol to DHA. A comparative study between differently sized Sb-promoted and unpromoted Pt/CNTs catalysts was carried out to decouple the Sb promoter effects from the metal size effects. The role of the Sb promoter was elucidated by combining multiple catalyst characterization techniques with density functional theory (DFT) calculations. Finally, the plausible catalyst structure-performance relationship was established.

Experimental

Catalyst preparation

Carbon nanotubes (purity > 99.8%, purchased from CNano Technology) with closed ends were used as catalysts support without further treatments, and their pores were mainly derived from the CNTs entanglement according to N_2 adsorption–desorption isotherm and SEM measurements (Figure S1, Supporting Information). The CNTs supported Pt–Sb bimetallic catalysts ($n_{Pt}:n_{Sb} = 1.04$) with different metal loadings were synthesized by incipient wetness co-impregnation method. Chloroplatinic acid (Sinopharm Chemical Reagent Co., Ltd.) and antimony trichloride (prepared by dissolving antimony(III) oxide in 12 mol/L HCl) were used as the metal precursors, which were dissolved in deionized water with an electrical conductivity $<10^{-6}$ S/cm. The impregnated samples were first dried in stagnant air at ambient temperature for 12 h,

and then dried at 393 K for 12 h in an oven. The dried samples were further reduced by a continuous H_2 flow (60 cm^3/min) at 673 K for 4 h. After being cooled to room temperature, the reduced catalysts were passivated by 1% O_2/Ar for 0.5 h. The as-obtained catalysts were denoted as mPt-nSb, in which m and n denote the nominal loadings (wt %) of Pt and Sb, respectively.

Catalyst characterization

N_2 adsorption–desorption isotherm was obtained on an ASAP 2010 system (Micromeritics, USA). The morphology of CNTs was characterized by scanning electron microscopy (SEM) on a NOVA Nano SEM450 (FEI, USA). High-angle annular dark-field scanning transmission electron microscopy (HAADF-STEM) images were obtained on a Tecnai G2 F20 S-Twin (FEI, USA) equipped with a digitally processed STEM imaging system. The energy dispersive X-ray (EDX) signals of the particles were obtained in STEM mode by focusing the electron beam on the individual particle. High resolution transmission electron microscopy (HRTEM) images were obtained on a JEM 2100F (JEOL, Japan) with accelerating voltage of 200 kV. The average particle size and distribution of catalysts were determined by measuring more than 150 randomly selected particles. X-ray photoelectron spectroscopy (XPS) was conducted on an Axis Ultra DLD spectrometer (Kratos, Japan) using Al Kα radiation (1486.6 eV). The binding energy of samples was calibrated using the binding energy of the C 1s peak (284.6 eV) as a reference.

Selective catalytic oxidation of glycerol

Glycerol oxidation was carried out at atmospheric pressure in a three-neck flask equipped with a magnetic stirrer, a condenser and a gas supply system, as depicted in Figure 1. Typically, 30 mL aqueous solution of glycerol (0.1 g/mL) and an appropriate amount of pre-reduced catalyst were added into the reactor in a well temperature-controlled water bath and heated to 60°C, where there is no obvious change in the reaction temperature during the whole reaction process. The slurry was stirred at a speed of 500 rpm, and O_2 was bubbled into the reactor at a flow rate of 150 cm^3/min via a mass flow controller, where the effects of external mass transfer limitations can be eliminated according to our previous work.[20] Moreover, the
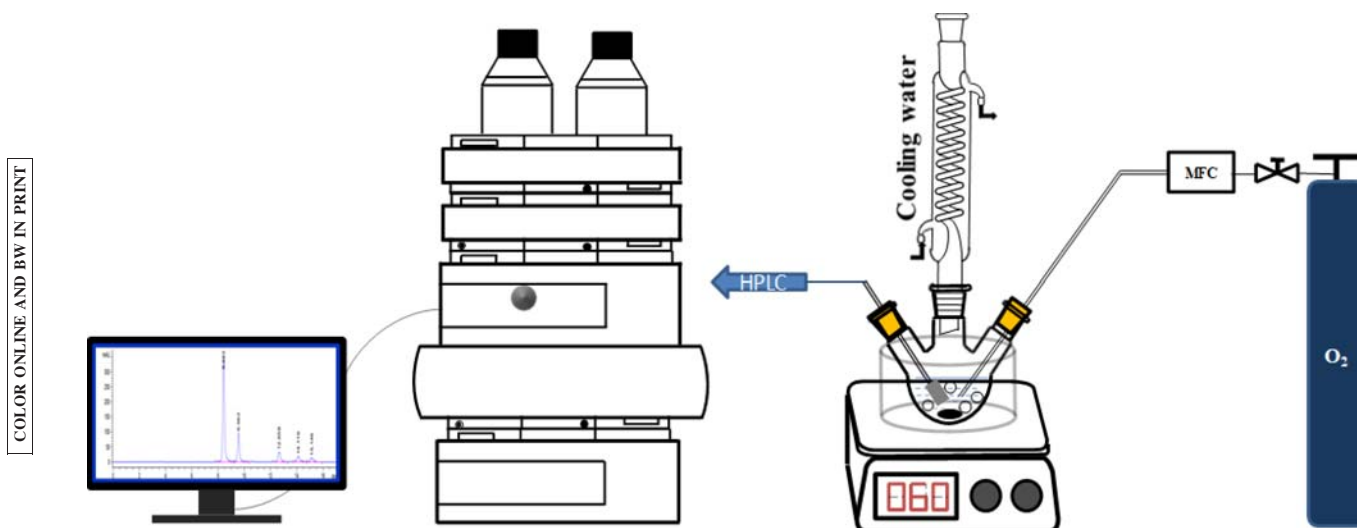
Figure 1. Scheme of the reaction vessel and attachments.

[Color figure can be viewed at wileyonlinelibrary.com]

effects of internal mass transfer limitations can also be ignored based on the unique pore characteristics of our used CNTs support mentioned above. During the reaction, the samples were drawn out intermittently from the reactor, filtered using 0.22 μm NY filters and then analyzed using a high performance liquid chromatograph (HPLC, Agilent 1100 series). The HPLC was equipped with a UV (210 nm) and a refractive index detector using a BP-OA column (300 × 7.8 mm) operating at 353 K. The eluent was an aqueous solution of H_3PO_4 (0.001 g/mL) operating at 0.5 mL/min. The reactant and products were quantified with external standard method.

DFT calculations

All periodic spin-polarized DFT calculations were performed with the generalized gradient approximation proposed by Perdew–Burke–Ernzerhof (PBE) using the Vienna Ab-initio Simulation Package (VASP). The interactions between ion cores and valence electrons were described by the projector augmented wave method, and the exchange-correlation function was GGA-PBE. The solution of the Kohn–Sham equations was expanded in a plane wave basis set with a cutoff energy of 400 eV. The sampling of the Brillouin zone was performed using a Monkhorst–Pack scheme, and electronic occupancies were determined in light of a Methfessel–Paxton scheme with an energy smearing of 0.2 eV.

We obtained a DFT-determined equilibrium lattice constant of 3.98 Å for bulk Pt in the face-centered-cubic (fcc) structure, which agrees well with the experimental bulk lattice constant (3.92 Å)[26] and other lattice constants reported in the literature for Pt.[27] Based on the calculated lattice constants, glycerol adsorptions were calculated on p (4 × 4) supercell slab with four-layered Pt(111) surfaces. For the calculation of surfaces and glycerol adsorption, bottom two-layered Pt were fixed and the top two-layered Pt as well as the adsorbates were relaxed. The Monkhorst–Pack mesh of 3 × 3 × 1 k-point sampling in the surface Brillouin zone was used. To minimize the interactions between the slabs, we employed a vacuum region with a 12 Å thickness. Since the XPS results show that Sb is mainly present as Sb oxide species on catalyst surface, a SbO-Pt(111) slab was also built based on the above Pt(111) surfaces with adsorbed SbO on the most stable site.

The adsorption energy (E_{ad}) is determined by Eq. 1.

$$E_{ad} = E_{Gly/slab} - E_{Gly} - E_{slab} \tag{1}$$

where $E_{Gly/slab}$, E_{Gly}, and E_{slab} are the energies of glycerol on the slab, glycerol in gas phase, and the slab, respectively.

Results and Discussion

Improved catalytic activity by Sb promoter

Various Pt–Sb/CNTs catalysts with different metal loadings but a constant Pt/Sb molar ratio were synthesized and then characterized by multiple techniques. Figure 2 shows typical HAADF-STEM image and EDX line-scanning profile across an individual particle of Pt–Sb/CNTs catalyst. Both Pt and Sb are observed to be distributed throughout the particle, indicating the coexistence of Pt and Sb in the metal nanoparticles over the Pt–Sb/CNTs catalyst. Different Pt–Sb/CNTs catalysts were characterized by HRTEM, and the results are shown in Figure 3. It is found that most of the Pt–Sb nanoparticles are highly dispersed on the CNTs support except the 8.0Pt–4.8Sb catalyst with the presence of some agglomerations, and their average particle sizes gradually increase from 2.1 to 3.4 nm. These differently sized Pt–Sb/CNTs catalysts were employed for selective base-free oxidation of glycerol to DHA. Figure 4 shows the glycerol conversion as a function of the metal particle size at a reaction time of 2 h, where the glycerol conversions over differently sized Pt/CNTs catalysts are taken from our previous studies.[20] This comparison allows us to understand the intrinsic role of Sb promoter by excluding the metal particle size effects, i.e., decoupling the Sb promoter effects from the metal size effects. Clearly, under similarly sized metal nanoparticles, the Pt–Sb/CNTs catalysts outperform much higher glycerol conversion than the Pt/CNTs catalyst, indicating that the Sb promoter has a remarkably promotional effect on the catalytic glycerol oxidation activity.

It can also be clearly seen in Figure 4 that both cases show remarkable size-dependent glycerol oxidation activity for CNTs supported Pt and Pt–Sb nanoparticles with the average size of 1.5–2.9 and 2.1–3.4 nm, respectively. For example, for the Pt-based catalysts with Sb promoter, the glycerol conversion rises significantly from 50 to 70% with the particle size
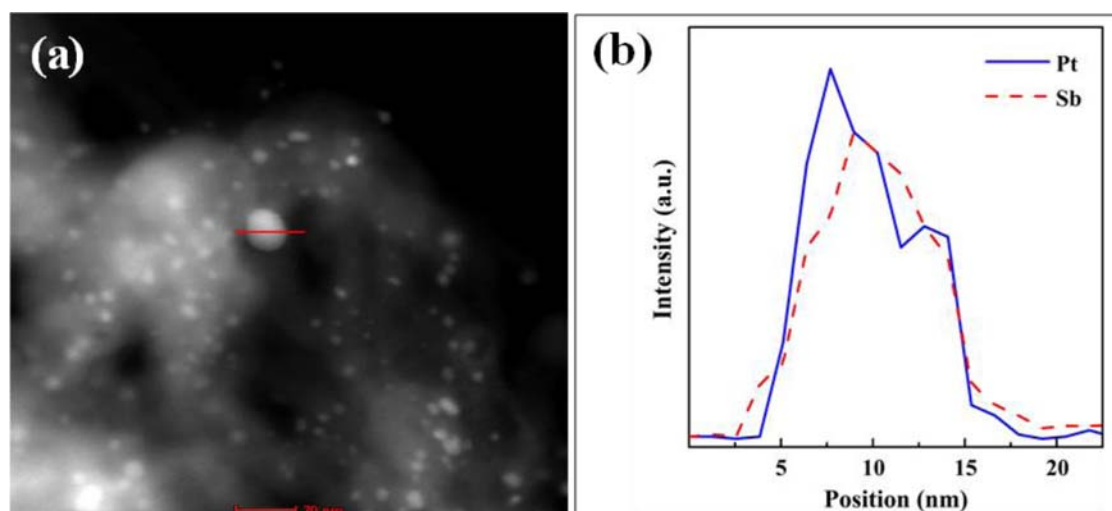
Figure 2. (a) Typical HAADF-STEM image and (b) EDX line-scanning profiles across an individual particle of Pt–Sb/CNTs catalyst.

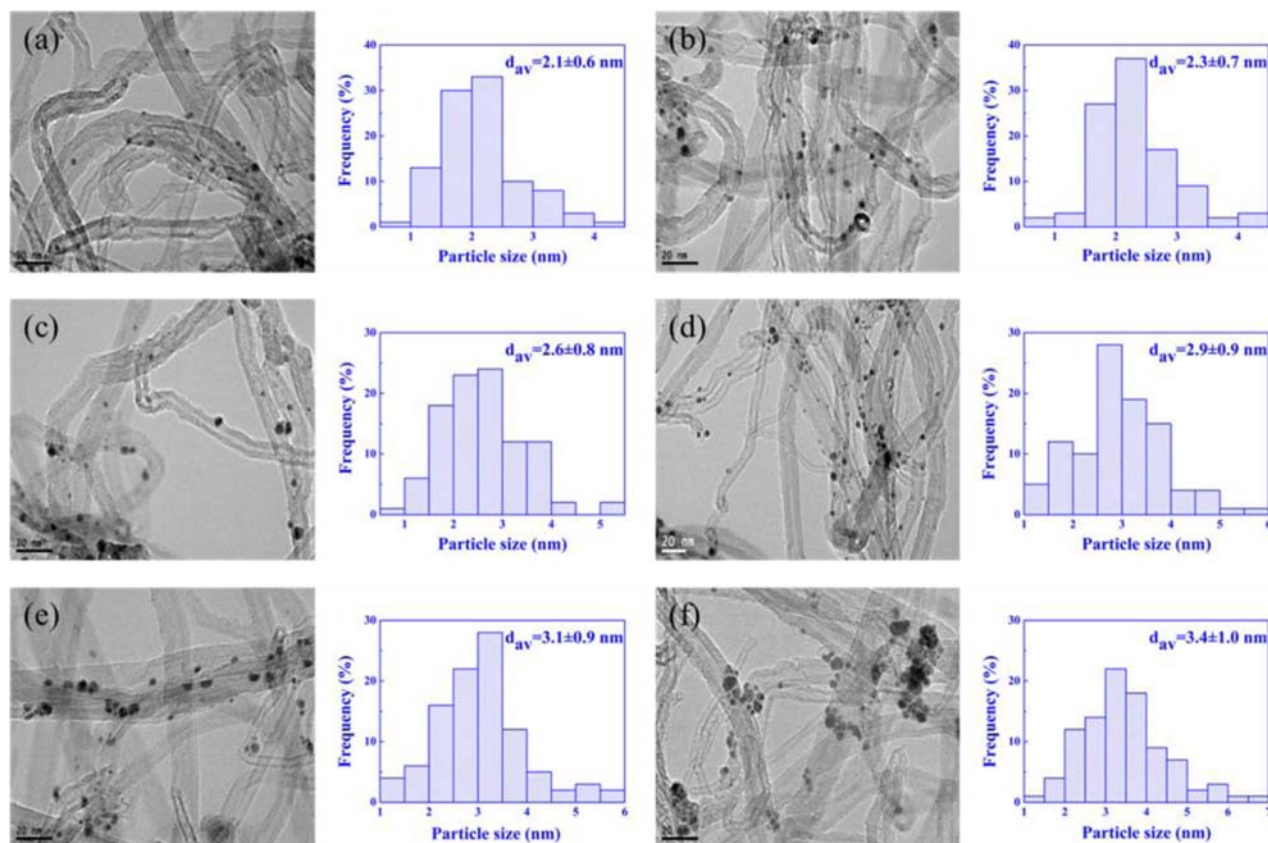[Color figure can be viewed at wileyonlinelibrary.com]

Figure 3. Typical HRTEM images and the corresponding particle size distribution histograms of Pt–Sb/CNTs catalysts: (a) 2.0Pt–1.2Sb, (b) 3.0Pt–1.8Sb, (c) 4.0Pt–2.4Sb, (d) 5.0Pt–3.0Sb, (e) 6.5Pt–3.9Sb, and (f) 8.0Pt–4.8Sb.

[Color figure can be viewed at wileyonlinelibrary.com]

227 increasing from 2.1 to 3.1 nm. For the Pt/CNTs catalysts, the
228 size effects are most likely ascribed to the difference in the
229 number of the active sites according to our previous stud-
230 ies,[28,29] where 1.5–2.9 nm sized Pt nanoparticles supported on

CNTs exhibit similar Pt binding energies, but remarkable 231
change in the number of each exposed surface atoms with the 232
metal particle size (Figure S2, Supporting Information). For 233
the Pt–Sb/CNTs catalysts, understanding of the size effects 234
will be shown below. 235

Tuning of product selectivity 236

In addition to the improved catalytic activity, the improve- 237
ment of the Sb promoter in the product selectivity is another 238
important issue for the base-free oxidation of glycerol. For the 239
reaction system involving some parallel and consecutive reac- 240
tions, it is necessary to plot the product selectivity with the 241
reactants conversion for a fair comparison.[30] As shown in Fig- 242
ure 5, under similar glycerol conversions, the Pt–Sb/CNTs cat- 243 F5
alysts appear to afford much more DHA, while the Pt/CNTs 244
catalyst with more GLYD and glyceric acid (GLYA), strongly 245
indicating that the Sb promoter endows the catalysts with the 246
selective oxidation of glycerol to form DHA. Notably, for dif- 247
ferently sized Pt–Sb/CNTs catalysts, the DHA selectivity 248
increases from ∼65% up to 90% with the particle size increas- 249
ing from 2.1 to 3.1 nm under similar glycerol conversions of 250
∼40%, and the typical size effects on other products selectiv- 251
ities are also observed. In other words, 2.1–3.4 nm sized Pt– 252
Sb/CNTs catalysts exhibit remarkable size-dependent product 253
selectivity for base-free glycerol oxidation. 254

It can also be seen in Figure 5 that over the Pt–Sb/CNTs cat- 255
alysts, increasing the glycerol conversion leads to the 256
decreased selectivity to DHA but increased ones to GLYD and 257
GLYA. To exclude the possibility for the formation of GLYD 258
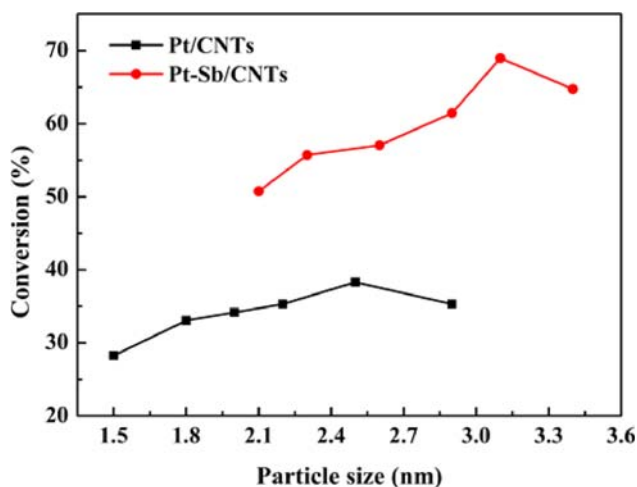and GLYA from the consecutive conversion of the generated 259

Figure 4. Glycerol conversion as a function of metal particle size over Pt-based catalysts at a reaction time of 2 h.

The data for the Pt/CNTs catalysts are taken from Ref. 20. Reaction conditions: 30 mL, 0.1 g/mL glycerol aqueous solution, glycerol/Pt molar ratio = 890, $T = 60°C$ and O_2 flow rate = 150 cm³/min. [Color figure can be viewed at wileyonlinelibrary.com]
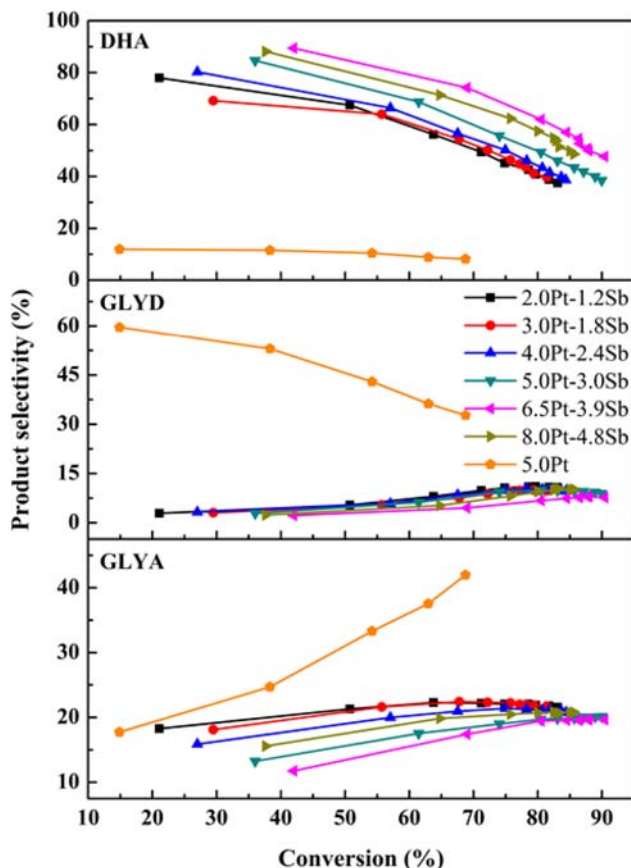
Figure 5. Product selectivity as a function of glycerol conversion over the Pt-based catalysts.

Reaction conditions: 30 mL, 0.1g/mL glycerol aqueous solution, glycerol/Pt molar ratio = 890, $T = 60°C$ and O_2 flow rate = 150 cm³/min. [Color figure can be viewed at wileyonlinelibrary.com]

and no detected DHA was observed. Based on the above analyses, the main reaction pathways for the glycerol oxidation over the Pt-based catalysts are schematically shown in Figure 6. Specifically, the Pt–Sb/CNTs catalysts favor the oxidation of the secondary glycerol hydroxyl group to form DHA (i.e., Route I), whereas the Pt/CNTs catalyst with the preferential oxidation of the primary glycerol hydroxyl group to form GLYD and GLYA (i.e., Route II). Therefore, the introduction of the Sb promoter is shown to be a very effective way to tame the Pt-catalyzed glycerol oxidation reaction toward the Route I.

Moreover, the ratio of the DHA selectivity to the GLYD and GLYA selectivities is further compared for the differently sized Pt–Sb/CNTs catalysts, as displayed in Figure 7a. Apparently, the selectivity ratio is relatively high for the largely sized Pt–Sb/CNTs catalysts, suggesting the favorable oxidation of the secondary hydroxyl group of glycerol to DHA over the larger one. This is in accordance with the yield of DHA over the differently sized Pt–Sb/CNTs catalysts shown in Figure 7b. As can be seen, largely sized Pt–Sb/CNTs catalysts offer a higher DHA yield, and there exists an optimal yield of DHA dependent on the reaction time, implying that more DHA can be produced by manipulating the particle size of Pt–Sb/CNTs catalysts and the reaction time. The dependence of the selectivity to C_3 products on the metal particle size is also compared, and the results are presented in Figure 7c. Clearly, the catalysts with the largely sized metal particles afford the increased C_3 products selectivity under the similar glycerol conversions, indicating the inhibited oxidative cleavage of the C–C bond. These unique reaction characteristics over the Pt–Sb/CNTs catalysts are also shown in Figure 6.

Plausible catalyst structure–performance relationship

As mentioned above, the comparative studies between the Sb-promoted and unpromoted Pt/CNTs catalysts have demonstrated the significantly promotional effects of Sb on the selective base-free oxidation of glycerol to DHA under excluding the metal particle size effects. This indicates that the difference in their electronic properties could be one important factor for the difference in their catalytic performances.[29] To understand this issue, the differently sized Pt–Sb/CNTs catalysts and Pt/CNTs one were characterized by XPS, and the

DHA, the base-free oxidation of DHA over the typical Pt–Sb/CNTs catalyst has been carried out in our previous work.[31] As expected, there are no detected GLYD and GLYA in the products. Moreover, when the GLYD was used as the reactant, the GLYA was discriminated as the dominant oxidation product,
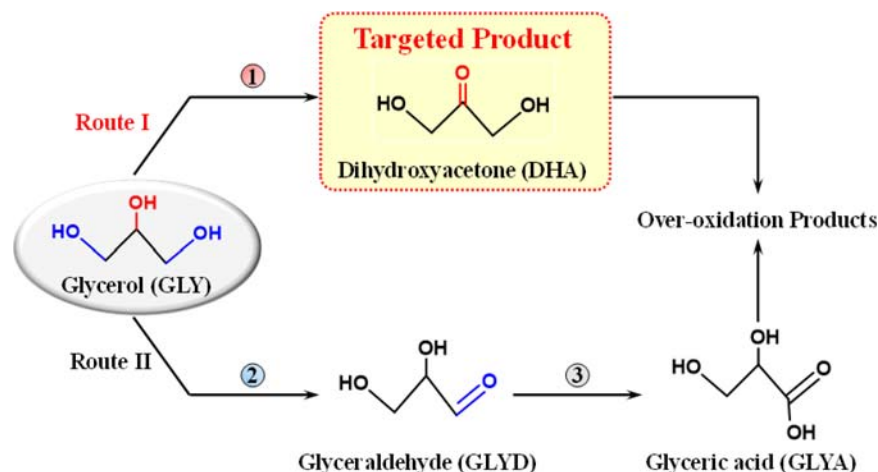
Figure 6. Possible reaction pathway for glycerol oxidation over Pt-based catalysts.

Note: Route I as the dominant reaction pathway over the Pt–Sb/CNTs catalyst especially for the largely sized ones which show the inhibited oxidative cleavage of the C–C bonds to form the over-oxidation products, and Route II as the dominant one over the Pt/CNTs catalyst. [Color figure can be viewed at wileyonlinelibrary.com]
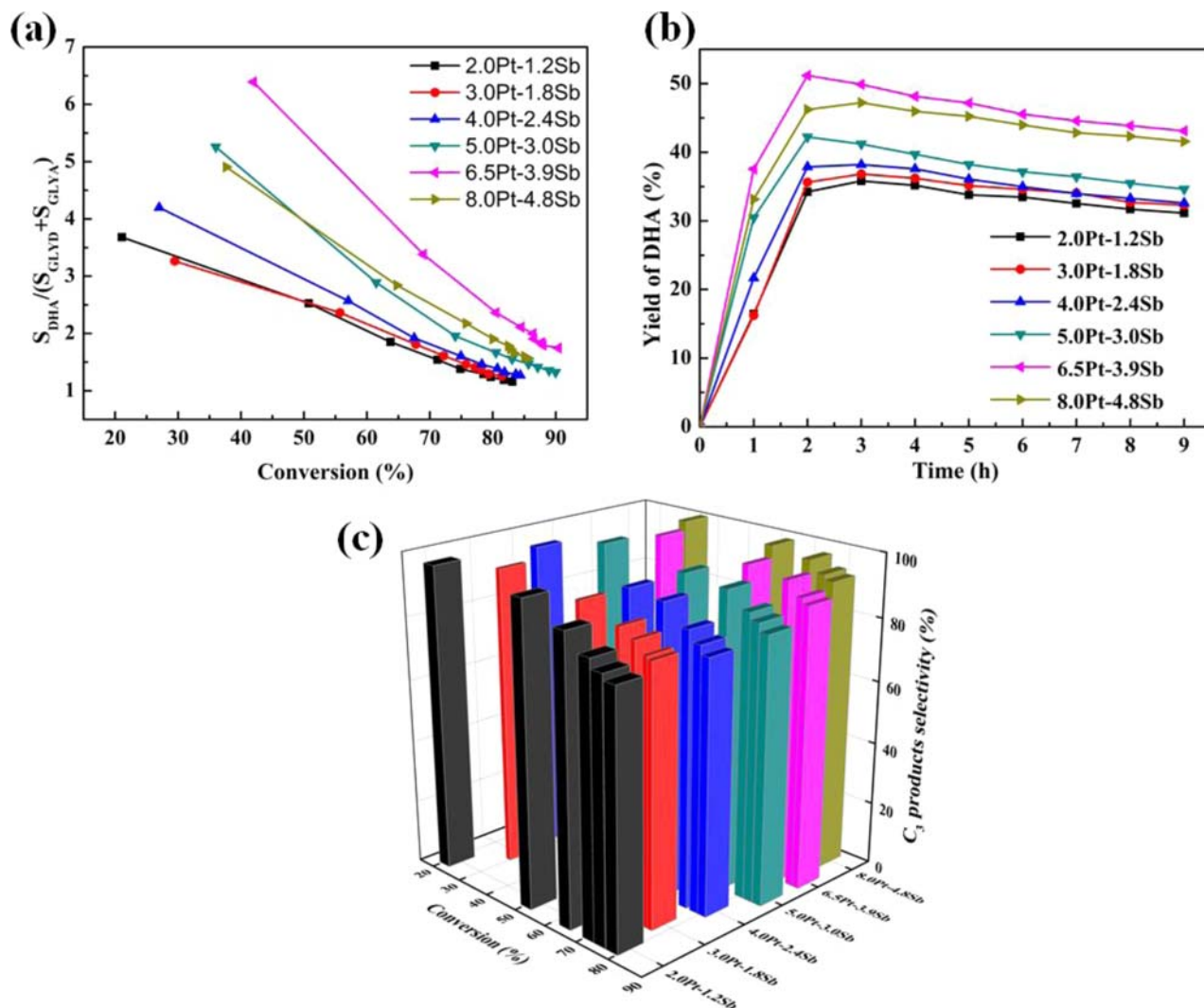
Figure 7. (a) Selectivity ratio for DHA/(GLYD + GLYA), **(b)** yield of DHA as a function of reaction time, and **(c)** C_3 products selectivity as a function of glycerol conversion over differently sized Pt–Sb/CNTs catalysts.

Reaction conditions: 30 mL, 0.1 g/mL glycerol aqueous solution, glycerol/Pt molar ratio = 890, $T = 60°C$ and O_2 flow rate = 150 cm^3/min. [Color figure can be viewed at wileyonlinelibrary.com]

results are shown in Figure 8. Each Pt 4f signal could be deconvoluted into three peaks.[22] The most intensive peaks are attributed to the Pt^0 $4f_{7/2}$ and Pt^0 $4f_{5/2}$, meaning that the Pt mainly exists in the form of metallic state. It can also be observed that the Pt^0 $4f_{7/2}$ binding energies for the Pt–Sb/CNTs catalysts (~71.8 eV) are slightly smaller than that for the Pt/CNTs catalyst (71.9 eV). According to our previous studies, the lower Pt^0 $4f_{7/2}$ binding energies have been reported to be unfavorable for the glycerol oxidation.[22] However, as mentioned above in Figure 4, the Pt–Sb/CNTs catalysts with the lower Pt^0 $4f_{7/2}$ binding energies show much higher glycerol oxidation rate than the Pt/CNTs catalysts. Therefore, it can be reasonably concluded that the different electronic properties cannot explain why the Pt–Sb catalysts exhibit much higher catalytic activity for the reaction.

Moreover, for the differently sized Pt–Sb/CNTs catalysts, their Pt^0 $4f_{7/2}$ binding energies are very similar, i.e., ~71.8 eV, which is difficult to explain the large difference in the DHA selectivity and yield. In other words, the tiny difference in the electronic properties of the differently sized Pt–Sb/CNTs catalysts are not main reason for the significantly different base-

free oxidation performance of glycerol. All of these results indicate that compared to the Pt/CNTs catalyst, the geometric effects of the Sb promoter over the Pt–Sb/CNTs catalysts could be dominant factor for the selective oxidation of glycerol to DHA. Notably, the deconvolution analyses of the Sb $3d_{5/2}$ XPS spectra overlapping with the O 1s spectra for the Pt–Sb/CNTs catalysts in Figure 8 reveal that the electronic properties of Sb are similar for all the catalysts and the main Sb peaks are ascribed to the $Sb^{\delta+}$. Therefore, for the Pt–Sb/CNTs catalysts, the Sb species are mainly in the form of Sb oxide species (i.e., SbO_x), which is most likely due to the strong oxophilic nature of the Sb.[32]

As a consecutive effort, DFT calculations were further performed to understand the SbO_x promotional effects. First, the Pt(111) and SbO-Pt(111) slabs were built, where the former one was used as a reference. The adsorption behaviors of glycerol on the two surfaces were comparatively studied, and the correspondingly stable adsorption configurations are presented in Figure 9. Very interestingly, on the clean Pt(111) surface, the glycerol molecule is adsorbed with the oxygen atom of the primary hydroxyl group binding to the Pt atom, whereas on
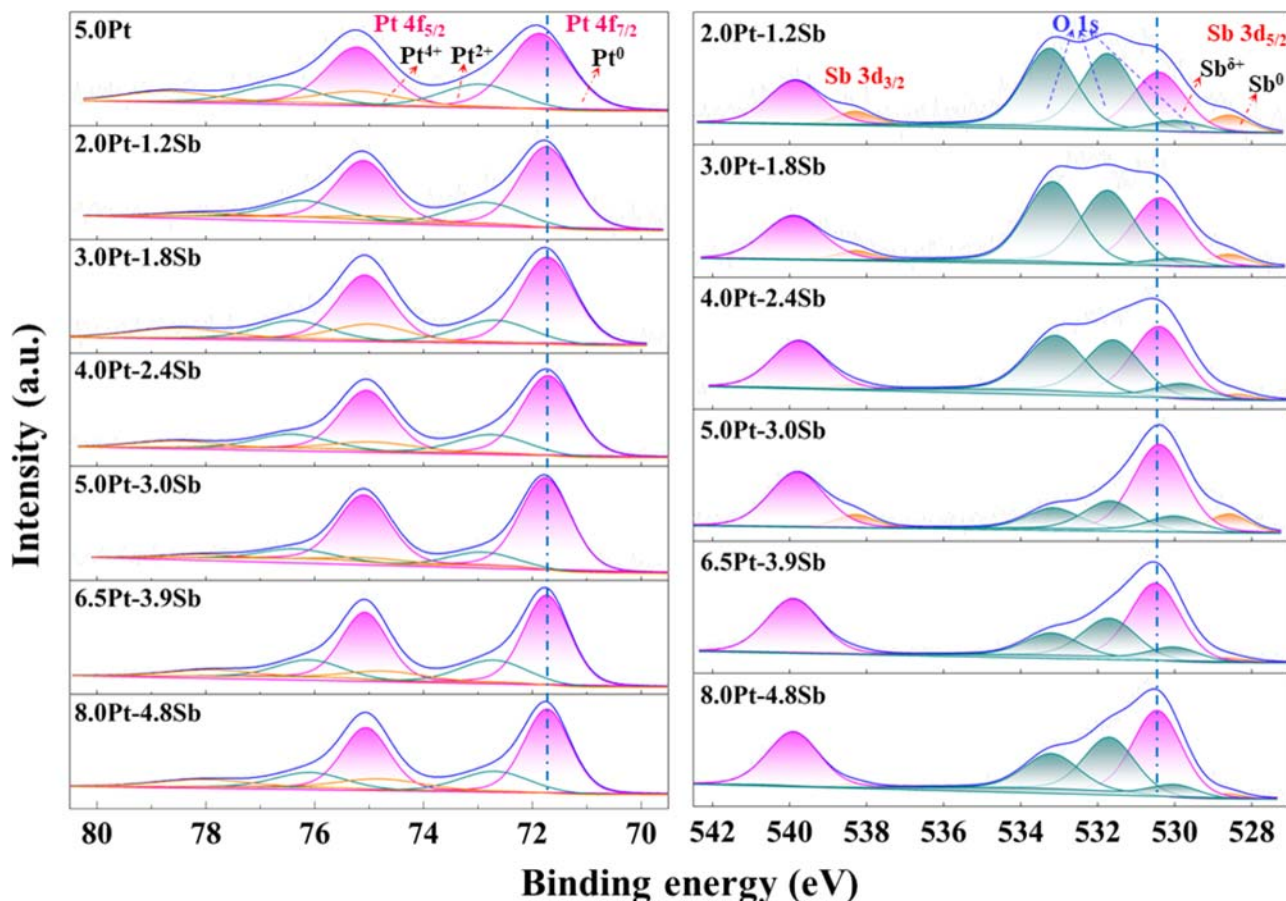
Figure 8. XPS spectra of Pt 4f and Sb 3d regions over Pt/CNTs and Pt–Sb/CNTs catalysts.

[Color figure can be viewed at wileyonlinelibrary.com]

the SbO-Pt(111) surface, besides the binding of the primary hydroxyl group, the oxygen atom of the secondary hydroxyl group also binds to the Sb atom; the SbO-Pt(111) surface shows slightly higher glycerol adsorption energy than the Pt(111) surface. We also observed some changes in the bond lengths of hydroxyl groups upon adsorption, as listed in Table
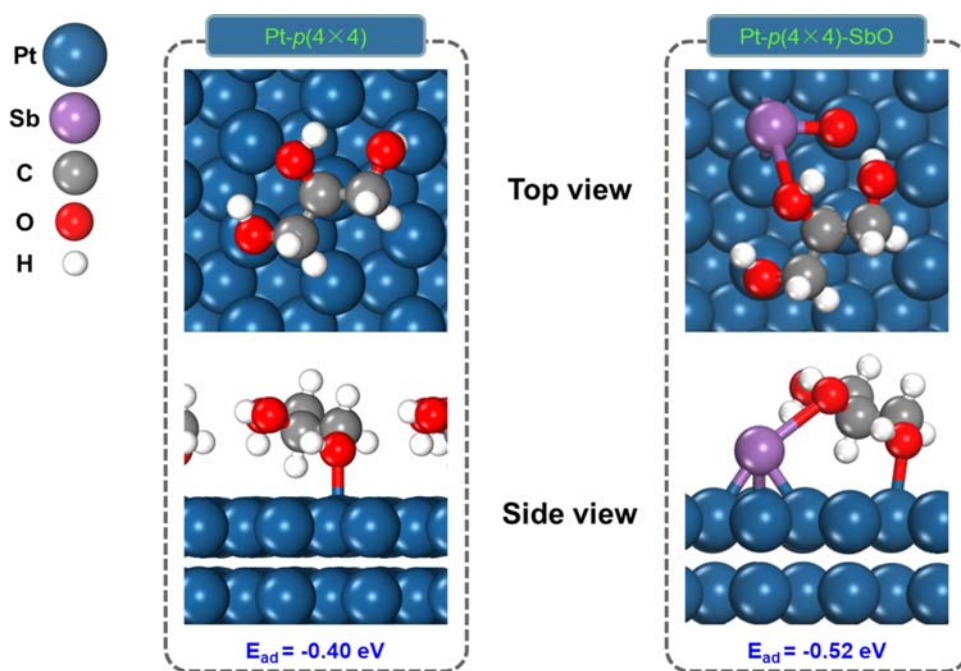

Figure 9. The lowest energy configurations of glycerol on Pt(111) and SbO-Pt(111) surfaces.

The numbers below correspond to the adsorption energy. [Color figure can be viewed at wileyonlinelibrary.com]

Table 1. Comparison of O–H Bond Length (in Å) Between the Glycerol (GLY) Molecule and the Configurations of Glycerol on Pt(111) and SbO-Pt(111) Surfaces

	GLY	GLY/Pt(111)	GLY/SbO-Pt(111)
Primary hydroxyl group	0.976	0.981	0.979
Secondary hydroxyl group	0.978	0.982	0.991

1. Both the primary and secondary hydroxyl groups have stretched to some extent due to the interaction of glycerol molecule with the Pt surfaces. Especially, the bond length of O—H in the secondary hydroxyl group increases from 0.978 to 0.991 Å with the adsorption of glycerol on the SbO-Pt(111) surface, which may lead to the preferential activation of the secondary hydroxyl group. Based on the theoretical analyses of glycerol adsorption on the two surfaces, the dominant promotional effects of the SbO_x on the DHA selectivity and yield could arise from the preferential adsorption configuration of glycerol, i.e., the favorable activation of the secondary hydroxyl group. More detailed theoretical studies on the Sb promotional effects are still ongoing in our group, which would be a very interesting subject to reveal the underlying reaction mechanism and guide the catalyst rational design and optimization.

Conclusions

The catalytic performances between differently sized SbO_x-promoted and unpromoted Pt/CNTs catalysts for base-free oxidation of glycerol to DHA have been comparatively studied, and the crucial role of the Sb promoter has been explored under excluding the metal particle size effects. Compared to the unpromoted Pt/CNTs catalysts, the SbO_x-promoted Pt/CNTs catalysts especially for largely sized ones exhibited improved catalytic activity and DHA selectivity as well as inhibited oxidative cleavage of the C–C bond. XPS measurements exhibited that the Sb species are mainly in the form of SbO_x, and the differently sized promoted catalysts possess similar metal binding energies. On the basis of the characterization results and DFT calculations, a plausible catalyst structure-performance relationship was established. The preferential adsorption configuration of glycerol rather than the electronic properties seems to be mainly responsible for the enhanced reaction activity and the DHA selectivity over promoted Pt/CNTs catalysts. These results clearly demonstrated the underlying promotional effects of the Sb promoter on the base-free oxidation of glycerol to DHA over the Pt-based catalysts, which could shed new light on the catalyst rational design and optimization.

Acknowledgments

Literature Cited

1. Zhou CH, Beltramini NJ, Fan YX, Lu GQ. Chemoselective catalytic conversion of glycerol as a biorenewable source to valuable commodity chemicals. *Chem Soc Rev*. 2008;37(3):527–549.

2. Katryniok B, Kimura H, Skrzyńska E, Girardon J-S, Fongarland P, Capron M, Ducoulombier R, Mimura N, Paul S, Dumeignil F. Selective catalytic oxidation of glycerol: perspectives for high value chemicals. *Green Chem*. 2011;13(8):1960–1979.

3. Kong PS, Aroua MK, Daud WMAW. Conversion of crude and pure glycerol into derivatives: a feasibility evaluation. *Renew Sust Energ Rev*. 2016;63:533–555.

4. Hirasawa S, Nakagawa Y, Tomishige K. Selective oxidation of glycerol to dihydroxyacetone over a Pd-Ag catalyst. *Catal Sci Technol*. 2012;2(6):1150–1152.

5. Ketchie WC, Murayama M, Davis RJ. Promotional effect of hydroxyl on the aqueous phase oxidation of carbon monoxide and glycerol over supported Au catalysts. *Top Catal*. 2007;44(1–2):307–317.

6. Zope BN, Hibbitts DD, Neurock M, Davis RJ. Reactivity of the gold/water interface during selective oxidation catalysis. *Science*. 2010;330(6000):74–78.

7. Carrettin S, McMorn P, Johnston P, Griffin K, Hutchings GJ. Selective oxidation of glycerol to glyceric acid using a gold catalyst in aqueous sodium hydroxide. *Chem Commun*. 2002;(7):696–697.

8. Villa A, Veith GM, Prati L. Selective oxidation of glycerol under acidic conditions using gold catalysts. *Angew Chem Int Ed*. 2010;49(26):4499–4502.

9. Tsuji A, Rao KTV, Nishimura S, Takagaki A, Ebitani K. Selective oxidation of glycerol by using a hydrotalcite-supported platinum catalyst under atmospheric oxygen pressure in water. *ChemSusChem*. 2011;4(4):542–548.

10. Xiao Y, Greeley J, Varma A, Zhao ZJ, Xiao GM. An experimental and theoretical study of glycerol oxidation to 1,3-dihydroxyacetone over bimetallic Pt-Bi catalysts. *AIChE J*. 2017;63(2):705–715.

11. Liang D, Gao J, Sun H, Chen P, Hou ZY, Zheng XM. Selective oxidation of glycerol with oxygen in a base-free aqueous solution over MWNTs supported Pt catalysts. *Appl Catal B Environ*. 2011;106(3–4):423–432.

12. Kimura H, Tsuto K, Wakisaka T, Kazumi Y, Inaya Y. Selective oxidation of glycerol on a platinum-bismuth catalyst. *Appl Catal A Gen*. 1993;96(2):217–228.

13. Garcia R, Besson M, Gallezot P. Chemoselective catalytic oxidation of glycerol with air on platinum metals. *Appl Catal A Gen*. 1995;127(1–2):165–176.

14. Carrettin S, McMorn P, Johnston P, Griffin K, Kiely CJ, Hutchings GJ. Oxidation of glycerol using supported Pt, Pd and Au catalysts. *Phys Chem Chem Phys*. 2003;5(6):1329–1336.

15. Ribeiro LS, Rodrigues EG, Delgado JJ, Chen XW, Pereira MFR, Orfao JJM. Pd, Pt, and Pt-Cu catalysts supported on carbon nanotube (CNT) for the selective oxidation of glycerol in alkaline and base-free conditions. *Ind Eng Chem Res*. 2016;55(31):8548–8556.

16. Dou J, Zhang BW, Liu H, Hong JD, Yin SM, Huang YZ, Xu R. Carbon supported Pt_9Sn_1 nanoparticles as an efficient nanocatalyst for glycerol oxidation. *Appl Catal B Environ*. 2016;180:78–85.

17. Zhu J, Holmen A, Chen D. Carbon nanomaterials in catalysis: Proton affinity, chemical and electronic properties, and their catalytic consequences. *ChemCatChem*. 2013;5(2):378–401.

18. Auer E, Freund A, Pietsch J, Tacke T. Carbons as supports for industrial precious metal catalysts. *Appl Catal A Gen*. 1998;173(2):259–271.

19. Chen WY, Duan XZ, Qian G, Chen D, Zhou XG. Carbon nanotubes as support in the platinum-catalyzed hydrolytic dehydrogenation of ammonia borane. *ChemSusChem*. 2015;8(17):2927–2931.

20. Lei JQ, Duan XZ, Qian G, Zhou XG, Chen D. Size effects of Pt nanoparticles supported on carbon nanotubes for selective oxidation of glycerol in a base-free condition. *Ind Eng Chem Res*. 2014;53(42):16309–16315.

21. Ning XM, Yu H, Peng F, Wang HJ. Pt nanoparticles interacting with graphitic nitrogen of N-doped carbon nanotubes: effect of electronic properties on activity for aerobic oxidation of glycerol and electro-oxidation of CO. *J Catal*. 2015;325:136–144.

22. Lei JQ, Dong H, Duan XZ, Chen WY, Qian G, Chen D, Zhou XG. Insights into activated carbon-supported platinum catalysts for base-free oxidation of glycerol. *Ind Eng Chem Res*. 2016;55(2):420–427.

23. Hu WB, Knight D, Lowry B, Varma A. Selective oxidation of glycerol to dihydroxyacetone over Pt-Bi/C catalyst: optimization of catalyst and reaction conditions. *Ind Eng Chem Res*. 2010;49(21):10876–10882.

24. Liang D, Cui SY, Gao J, Wang JH, Chen P, Hou ZY. Glycerol oxidation with oxygen over bimetallic Pt-Bi catalysts under atmospheric pressure. *Chin J Catal*. 2011;32(11–12):1831–1837.

25. Nie RF, Liang D, Shen L, Gao J, Chen P, Hou ZY. Selective oxidation of glycerol with oxygen in base-free solution over MWCNTs supported PtSb alloy nanoparticles. *Appl Catal B Environ*. 2012;127:212–220.

T1

26. Kittel C. *Introduction to Solid State Physics*, 7th ed. New York: John Wiley & Sons, Inc., 1996.

27. Tereshchuk P, Chaves AS, Da Silva JLF. Glycerol adsorption on platinum surfaces: a density functional theory investigation with van der Waals corrections. *J Phys Chem C*. 2014;118(28):15251–15259.

28. Chen WY, Ji J, Feng X, Duan XZ, Qian G, Li P, Zhou XG, Chen D, Yuan WK. Mechanistic insight into size-dependent activity and durability in Pt/CNT catalyzed hydrolytic dehydrogenation of ammonia borane. *J Am Chem Soc*. 2014;136(48):16736–16739.

29. Chen WY, Ji J, Duan XZ, Qian G, Li P, Zhou XG, Chen D, Yuan WK. Unique reactivity in Pt/CNT catalyzed hydrolytic dehydrogenation of ammonia borane. *Chem Commun*. 2014;50(17):2142–2144.

30. van der Wijst C, Duan XZ, Liland IS, Walmsley JC, Zhu J, Wang AQ, Zhang T, Chen D. ZnO-carbon-nanotube composite supported nickel catalysts for selective conversion of cellulose into vicinal diols. *ChemCatChem*. 2015;7(18):2991–2999.

31. Dong H, Lei JQ, Duan XZ, Qian G, Zhou XG. Reaction pathways for glycerol oxidation over carbon nanotubes supported Pt based catalysts (In Chinese). *Chem React Eng Technol*. 2016;32: 217–223.

32. Yu XW, Pickup PG. Codeposited PtSb/C catalysts for direct formic acid fuel cells. *J Power Sources*. 2011;196(19):7951–7956.